Chapter 3

Crystal and molecular structure of bis[(1-*p*-*n*-heptylphenyl, 3-*p*-*n*-heptyloxyphenyl) propane -1,3-dionato] copper(II)

3.1 Introduction

In this series, bis[(1-*p*-*n*-heptylphenyl, 3-*p*-*n*-heptyloxyphenyl)propane-1,3- dionato] copper(II), hereafter referred to as Cu-OC_7H_{15}-C_7H_{15}, is the only complex with dissimilarly substituted ligand *i.e.*, in Figure 1.6, the substitutions R_1 to R_4 are not identical. In Cu-OC_7H_{15}-C_7H_{15}, two of the four substituents are heptyloxy chains and the other two are heptyl chains. Such an asymmetry permits two types of geometric isomers *viz.*, those corresponding to the *trans* and the *cis* arrangements of the similar substituents with respect to the core shown in Figure 3.1(a) and (b) respectively. Also, with two alkyl and two alkoxy chains, the molecule of Cu-OC_7H_{15}-C_7H_{15} includes two oxygen atoms in the fringe around the core. It may be pointed out that in Cu-OC_8H_{17}, the crystal structure of which was described in the previous chapter, there are four oxygen atoms in the molecular fringe. The ensuing three chapters of this thesis describe the crystal structures of complexes with no oxygen atoms around the core. Thus, Cu-OC_7H_{15}-C_7H_{15} forms an interesting intermediate between complexes with four oxygen atoms and none respectively, around the core. The crystal structure analysis of Cu-OC_7H_{15}-C_7H_{15} is thus expected to provide information concerning the molecular conformation *i.e.*, occurrence of either the *trans* or the *cis* isomer and in addition enable identification of the possible effects of both dissimilar substitution and the presence of two oxygen atoms around the core, on the structural characteristics.

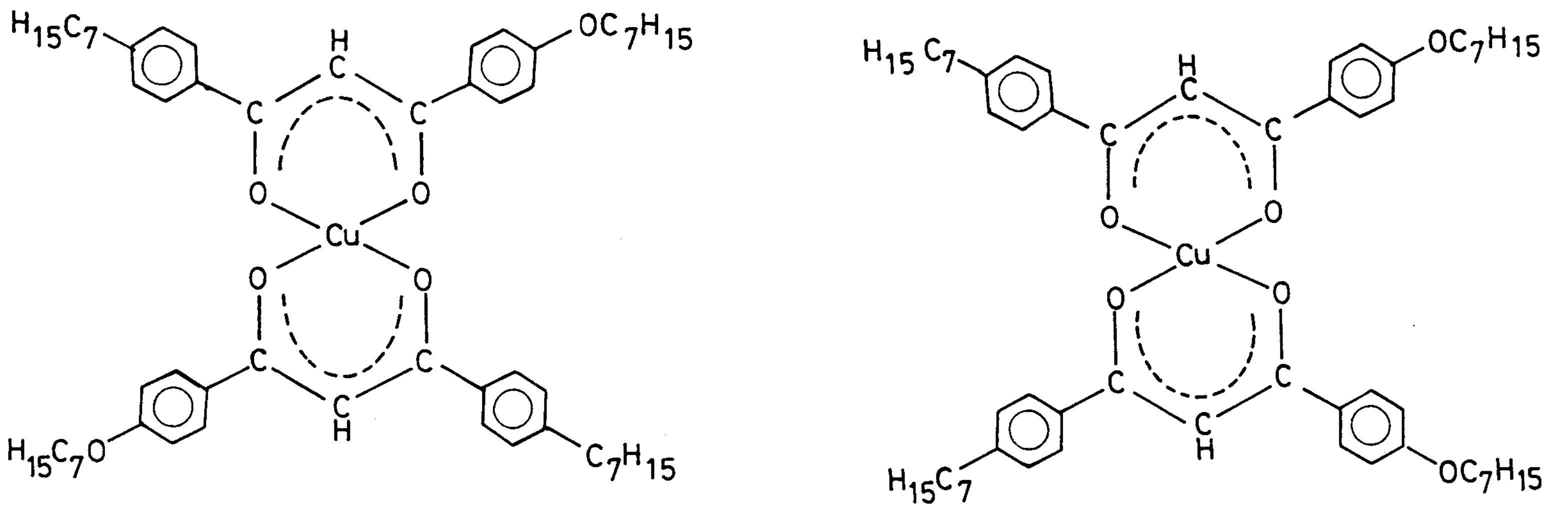

(a)

(b)

Figure 3.1: The geometric isomers of Cu-OC$_7$H$_{15}$-C$_7$H$_{15}$. **(a)** *trans* (b) *cis*

3.2 Experimental details

On heating, the complex Cu-OC_7H_{15}-C_7H_{15} was found to exhibit the following transitions [Prasad and Sadashiva, 1991] :

$$\begin{tikzcd}
C \arrow[rr, "150.3^\circ C"] & & I \arrow[dl, "145.5"] \\
& D &
\end{tikzcd}$$

where D refers to a discotic mesophase.

These transitions represent the occurrence of a monotropic mesophase *i.e.*, on heating, the crystal melts into a liquid and on cooling the liquid, the mesophase is observed before crystallization.

Transparent, green coloured prismatic single crystals of Cu-OC_7H_{15}-C_7H_{15} were obtained by slow evaporation from a solution in butan-2-one. Preliminary characterization of the crystal done using oscillation and Weissenberg photographs showed that the crystal belongs to the triclinic crystal system. The unit cell dimensions were, however, determined and refined by least squares method on a CAD4 single crystal diffractometer using 25 reflections in the θ range 10 to 29°. Three dimensional intensity data were collected on the same diffractometer using a crystal of approximate dimensions 0.6x0.1x0.1 mm^3, CuK_α radiation and in the $\omega/2\theta$ scan mode with a prescan speed of 5.5°/minute. Again, as described in Chapter 2, the final scan speed was, however, varied for each reflection to satisfy the relation, $\frac{\sigma(I)}{I} \leq 0.03$ where $\sigma(I)$ is the estimated standard deviation for the measured intensity, I. During data collection, the reflections $\bar{6}4\bar{1}$, $\bar{2}2\bar{1}$ and $\bar{4}4\bar{1}$ were used for both orientation and intensity control. Their intensities were checked once in every 3600 seconds. In the θ range of 1 to 55°, intensities of 6595 independent reflections were measured, of which only 2112 reflections had $I \geq 3\sigma(I)$. The intensities were corrected for Lorentz and polarization factors. Corrections for absorption effect was applied using the method of North et *al*, [1968]. Tables 3.1 and 3.2 present the crystal data and other relevant details of intensity data collection respectively.

As in the case of Cu-OC$_8$H$_{17}$ (Chapter 2), the crystal of Cu-OC$_7$H$_{15}$-C$_7$H$_{15}$ was also found to dissolve in most of the commonly available liquids. For reasons mentioned in Chapter 2, the density of this crystal (and the rest of the crystals discussed in the ensuing chapters) was not measured.

3.3 Structure determination and refinement

The value of calculated density, ρ_{calc}, assuming one molecule in the unit cell was very low (0.58 gm/cc). With two molecules in the unit cell, the ρ_{calc} value of 1.158 gm/cc was close to that observed for Cu-OC$_8$H$_{17}$ (1.163 gm/cc). Based on the statistical distribution of the normalized structure factors, E_{hkl}'s, shown in Table 3.3, the space group was chosen as $P\bar{1}$. It must be pointed out that the distribution of E_{hkl}'s is close to hypercentric. The asymmetric part of the cell therefore contains one formula unit of Cu-OC$_7$H$_{15}$-C$_7$H$_{15}$ *i.e.*, one copper atom, 64 other nonhydrogen atoms and 78 hydrogen atoms.

The crystal structure was solved using the direct methods program MULTAN-80 [Germain et *al*, 1971]. 480 reflections with E values $\geq$1.769 and 100 reflections corresponding to lowest E values were used to set up the phase relationships. It

Table 3.1: Crystal data.

Molecular formula	$C_{58}H_{78}O_6Cu$
Molecular weight	934.7
a	10.228(7) Å
b	16.607(5) Å
c	18.273(6) Å
α	64.40(2) °
β	78.53(6) °
γ	72.66(5) °
V	2663Å^3
Space group	PI
Z	2
ρ_{calc}	1.158 gm/cc
μ_{CuK_α}	9.548 cm^{-1}
$F_{(000)}$	1006

Table 3.2: Details of data collection.

Radiation used	CuK$_\alpha$
Crystal size	0.6×0.1×0.1 mm^3
Scan mode	$\omega/2\theta$
Maximum Bragg angle	55°
Number of unique reflections	6595
Number of reflections with $I \geq 3\sigma(I)$	2112
Ranges of h	0 to 10
k	-16 to 17
l	-18 to 19

Table 3.3: Distribution of the normalized structure factors.

Average	Experimental	Theoretical		
	all data	acentric	centric	hypercentric
$\|E\|$	0.697	0.886	0.798	0.718
E^2	1.000	1.000	1.000	1.000
E^3	2.305	1.329	1.596	1.916
E^4	6.387	2.000	3.000	4.500
E^5	31.963	3.323	6.383	12.260
E^6	223.851	6.000	15.000	37.500
$\|E^2-1\|$	1.096	0.736	0.968	1.145
$(E^2-1)^2$	5.387	1.000	2.000	3.500
$(E^2-1)^3$	20G.690	2.000	8.000	26.000

must be mentioned that the reflection 220, had the highest E value of **9.925,** the correlation of which with the molecular arrangement will be described later in this chapter. Details of the three origin defining reflections and the six reflections which formed the starting set are listed in Table 3.4. It may be noted that the reflection 2$\bar{2}$0 is part of the starting set.

With six reflections in the starting set, there are 2^6(=64) solutions. A summary of the figures of merit output by the tangent formula is presented in Table 3.5. The molecule could not be identified from the E-map corresponding to the best set, i.e., the set with the highest value of combined figure of merit, COMFOM of 2.24. The E-map corresponding to the set with the lowest R-value and the highest value of ABSFOM (*i.*e., set 1) did not also enable identification of the molecule. Examination of the E-maps from the other sets led to the identification of the copper atom and 49 other nonhydrogen atoms from set 6 *i.*e., corresponding to the eighth best COMFOM, second best R_{Karle} and third best ABSFOM. The PSIZERO value for this set was, however, 4.57.

Positional and isotropic thermal parameters of these 50 atoms were refined by blocked full matrix least squares procedure using the program SHELX-76 [Sheldrick, 1976]. The atomic parameters to be refined were divided into five blocks described in Table **3.6.** The initial R-factor of 0.415 reduced to 0.341 in four cycles of least squares refinement. From a difference electron density map computed at this stage, positions of 13 out of the remaining 15 atoms were identified, on inclusion of which the R-factor reduced to 0.237 in four cycles. It must be pointed out that the two atoms which were yet to be identified were the

Table **3.4:** Details of the origin defining and the starting set of reflections.

h	k	l	E_{hkl}	
5	12	9	7.391	origin
4	6	1	5.976	origin
2	$\bar{3}$	0	3.776	origin
2	$\bar{2}$	0	9.925	starting set
5	7	$\bar{4}$	4.285	starting set
1	$\bar{6}$	$\bar{15}$	4.052	starting set
1	$\bar{5}$	$\bar{17}$	3.869	starting set
2	10	$\bar{5}$	3.698	starting set
3	8	$\bar{2}$	3.572	starting set

Table 3.5: Summary of the figures of merit (FOM) output by the tangent formula.

	ABS FOM	PSI ZERO	R_{Karle}	COM FOM
Maximum value	1.1357	4.679	15.84	2.2396
Minimum value	0.8572	1.644	5.49	0.5260
Relative weights for COM FOM	0.60	1.20	1.20	

Table 3.6: Details of the blocking used in the least squares refinement.*

Block number	Positional and thermal parameters of the atoms constituting
1	core
2	Phenyl ring A and chain A
3	Phenyl ring B and chain B
4	Phenyl ring C and chain C
5	Phenyl ring D and chain D

*For nomenclature please refer to Figure **3.2** terminal atoms in the chains. From a difference electron density map computed at this stage, these two atoms could also be identified.

Until this stage, no distinction was made between the carbon and the oxygen atoms in the chains; all the atoms in the chains were treated as carbon atoms. Examination of the molecule showed that two of the chains had eight atoms each and these were identified as the heptyloxy chains. In the former set, the atoms bonded to the phenyl ring at the respective *para* positions were henceforth treated as oxygen atoms. After four cycles of least squares refinement, with all the 65 non-hydrogen atoms, the R-factor reduced to 0.208. Introduction of anisotropic thermal parameters and also weighting function described in Table 3.7, the R-factor further reduced to 0.096. At this stage of refinement, all the hydrogen atoms in the molecule were fixed geometrically, using a C-H distance of 1.08Å [International Tables for X-ray Crystallography, 1968]. The hydrogen atoms were assigned the isotropic temperature factors, U_{iso}, same as those of the equivalent isotropic thermal parameters, U_{eq}, of the respective carbon atoms to which they were bonded. The positional and the thermal parameters of the hydrogen atoms were not refined but their contribution to the structure factors were included during refinement. The refinement was terminated after five cycles, when all the shifts, Δ's were less than the corresponding e.s.d's, σ's. In the terminal cycle, the highest value of Δ/σ was 0.21 for the parameter U_{33} of the atom C(55) (Figure 3.2). The final R-value was 0.081 and the weighted R-factor (R_w) was 0.085 for 2119 independent reflections with $I \geq 3\sigma(I)$ (Table 3.7).

Table 3.7: Some details of the refinement.

Weighting scheme	$K/\sigma^2(F_o)+g(F_o^2)$
K	3.0192
g	0.00116
It for 2112 reflections with $I \geq 3\sigma(I)$	0.0812
R_w	0.0849
Maximum shift/e.s.d (Δ/σ)	0.21
Residual electron density	
ρ_{min}	-0.31 el/Å^3
ρ_{max}	0.32 el/Å^3

The residual electron density map was quite featureless, the maximum and minimum density being 0.32 and -0.31el/Å^3 respectively. For carbon and oxygen atoms, the scattering factors given by Cromer and Mann [1968] were used; for hydrogen atoms, values of Stewart *et al* [1965] were used. In the case of the metal atoms (Cu/Pd/Ni as specified in each chapter) the scattering factor given by Cromer and Waber [1965] were used. They were also corrected for anomalous scattering effects [Cromer and Liberman, 1970].

3.4 Results and discussion

The copper atom which forms the centre of the molecule occupies a general position. The positional and equivalent isotropic thermal parameters , U_{eq}, of all the nonhydrogen atoms are listed in Table 3.8. The anisotropic thermal parameter has the form,

$$exp\left[-2\pi^2(U_{11}h^2a^{*2} + U_{22}k^2b^{*2} + U_{33}l^2c^{*2} + 2U_{12}hka^*b^* + 2U_{13}hla^*c^* + 2U_{23}klb^*c^*)\right].$$

The U_{ij} values are recorded in Table 3.9. Table 3.10 contains the positional and the isotropic thermal parameters of all the hydrogen atoms.

The U_{eq} values in Table 3.8 show that as in the crystal structure of Cu-OC_8H_{17} (Chapter 2 of this thesis), on moving outward from the core to the fringe , there is a progressive increase in the thermal parameters. The average U_{eq} value of the 11 atom core is 0.084(5)Å^2. The average U_{eq} values of 0.08(1) and 0.08(1)Å^2 for the phenyl rings A and B respectively (Figure 3.2) are not significantly different from that of the core. In contrast, the average U_{eq} values of 0.10(1) and 0.10(1)Å^2 for the phenyl rings C and D indicate slightly larger

Table **3.8:** Fractional coordinates and the U_{eq}($Å^2$) values of nonhydrogen atoms. The quantities in the parantheses are the respective e.s.d's.

Atom	x	y	z	U_{eq}	Atom	x	y	z	U_{eq}
Cu	0.6011(2)	0.3739(1)	0.3963(1)	0.081(1)	C(33)	0.765(2)	0.554(1)	0.8309(9)	0.10(1)
O(1)	0.610(1)	0.3924(6)	0.4889(5)	0.091(6)	C(34)	0.843(2)	0.630(1)	0.8033(9)	0.10(1)
O(2)	0.496(1)	0.2825(6)	0.4558(5)	0.093(5)	C(35)	0.877(2)	0.639(1)	0.877(1)	0.13(1)
O(3)	0.5997(9)	0.3545(6)	0.3021(5)	0.079(5)	C(36)	0.947(2)	0.719(1)	0:847(1)	0.15(1)
O(4)	0.708(1)	0.4618(6)	0.3401(5)	0.088(5)	C(37)	0.978(2)	0.729(2)	0.913(1)	0.20(2)
C(5)	0.564(2)	0.354(1)	0.559(1)	0.083(9)	C(38)	0.037(2)	0.807(2)	0.893(1)	0.17(2)
C(6)	0.484(1)	0.287(1)	0.5850(8)	0.081(9)	C(39)	0.386(2)	0.1778(9)	0.558(1)	0.077(8)
C(7)	0.460(1)	0.2547(9)	0.5315(8)	0.084(S)	C(40)	0.324(2)	0.143(1)	0.634(1)	0.10(1)
C(8)	0.651(2)	0.397(1)	0.2286(9)	0.090(9)	C(41)	0.256(2)	0.075(1)	0.6568(9)	0.10(1)
C(9)	0.727(1)	0.4650(9)	0.2091(8)	0.076(8)	C(42)	0.251(2)	0.031(1)	0.609(1)	0.09(1)
C(10)	0.749(1)	0.491(1)	0.263(1)	0.083(9)	C(43)	0.319(2)	0.066(1)	0.531(1)	0.10(1)
C(11)	0.833(1)	0.5630(8)	0.2412(9)	0.067(8)	C(44)	0.381(2)	0.139(1)	0.506(1)	0.11(1)
C(12)	0.890(2)	0.603(1)	0.1603(8)	0.078(9)	C(45)	0.187(2)	-0.043(1)	0.6308(9)	0.11(1)
C(13)	0.969(2)	0.663(1)	0.1434(9)	0.10(1)	C(46)	0.182(2)	-0.078(1)	0.570(1)	0.11(1)
C(14)	0.981(2)	0.693(1)	0.2051(9)	0.090(9)	C(47)	0.102(2)	-0.153(1)	0.600(1)	0.12(1)
C(15)	0.920(2)	0.653(1)	0.2816(9)	0.080(8)	C(48)	0.098(2)	-0.183(1)	0.5342(9)	0.101(9)
C(16)	0.844(1)	0.5895(9)	0.2959(7)	0.076(8)	C(49)	0.022(2)	-0.261(1)	0.561(1)	0.12(1)
O(17)	0.064(1)	0.7530(6)	0.1792(6)	0.110(6)	C(50)	0.013(2)	-0.292(1)	0.498(1)	0.13(1)
C(18)	0.084(2)	0.780(1)	0.2432(8)	0.096(9)	C(51)	-0.061(2)	-0.369(1)	0.522(1)	0.16(1)
C(19)	0.166(2)	0.853(1)	0.205(1)	0.12(1)	C(52)	0.630(1)	0.368(1)	0.1659(9)	0.075(8)
C(20)	0.187(2)	0.882(1)	0.2718(9)	0.099(9)	C(53)	0.590(2)	0.287(1)	0.1902(9)	0.11(1)
C(21)	0.275(2)	0.951(1)	0.236(1)	0.12(1)	C(54)	0.565(2)	0.256(1)	0.136(1)	0.12(1)
C(22)	0.278(2)	0.984(1)	0.300(1)	0.14(1)	C(55)	0.580(2)	0.306(1)	0.0550(9)	0.10(1)
C(23)	0.372(3)	0.055(1)	0.255(1)	0.19(2)	C(56)	0.623(2)	0.385(1)	0.0295(9)	0.10(1)
C(24)	0.380(2)	0.087(1)	0.313(1)	0.18(1)	C(57)	0.647(2)	0.418(1)	0.082(1)	0.11(1)
C(25)	0.584(1)	0.3813(8)	0.6225(8)	0.064(7)	C(58)	0.557(2)	0.280(1)	-0.0037(8)	0.13(1)
C(26)	0.546(1)	0.3473(9)	0.7041(8)	0.078(8)	C(59)	0.464(2)	0.221(1)	0.015(1)	0.12(1)
C(27)	0.572(1)	0.3765(9)	0.7551(7)	0.073(8)	C(60)	0.440(2)	0.197(1)	-0.048(1)	0.14(1)
C(28)	0.647(2)	0.446(1)	0.725(1)	0.10(1)	C(61)	0.347(2)	0.130(1)	-0.027(1)	0.13(1)
C(29)	0.689(1)	0.4819(9)	0.6427(9)	0.087(8)	C(62)	0.325(2)	0.103(2)	-0.085(1)	0.16(2)
C(30)	0.658(1)	0.4474(9)	0.5942(7)	0.069(8)	C(63)	0.225(3)	0.037(2)	-0.054(2)	0.21(2)
O(31)	0.667(1)	0.4684(7)	0.7861(6)	0.099(6)	C(64)	0.204(3)	0.000(2)	-0.104(1)	0.22(2)
C(32)	0.741(2)	0.540(1)	0.7570(8)	0.096(9)					

Table 3.9: Anisotropic thermal parameters U_{ij}

Atom	U_{11}	U_{22}	U_{33}	U_{23}	U_{13}	U_{12}
Cu	0.090(2)	0.094(2)	0.070(1)	-0.033(1)	-0.004(1)	-0.037(1)
O(1)	0.124(9)	0.103(8)	0.049(6)	-0.016(6)	-0.010(6)	-0.053(7)
O(2)	0.121(9)	0.090(7)	0.062(6)	-0.008(5)	-0.005(6)	-0.054(6)
O(3)	0.098(8)	0.097(7)	0.059(6)	-0.034(6)	0.005(6)	-0.049(6)
O(4)	0.132(9)	0.090(7)	0.060(6)	-0.036(6)	0.001(6)	-0.048(6)
C(5)	0.10(1)	0.06(1)	0.10(1)	-0.04(1)	-0.02(1)	-0.01(1)
C(6)	0.10(1)	0.11(1)	0.07(1)	-0.07(1)	-0.026(9)	0.00(1)
C(7)	0.09(1)	0.07(1)	0.043(9)	0.019(8)	-0.006(9)	-0.015(9)
C(8)	0.10(1)	0.08(1)	0.07(1)	-0.028(9)	-0.02(1)	0.01(1)
C(9)	0.09(1)	0.07(1)	0.07(1)	-0.025(8)	0.009(9)	-0.05(1)
C(10)	0.07(1)	0.11(1)	0.09(1)	-0.07(1)	0.00(1)	0.002(9)
C(11)	0.07(1)	0.07(1)	0.09(1)	-0.062(9)	-0.018(9)	-0.005(8)
C(12)	0.11(1)	0.09(1)	0.06(1)	-0.056(9)	0.004(9)	-0.03(1)
C(13)	0.12(1)	0.10(1)	0.08(1)	-0.04(1)	0.00(1)	-0.04(1)
C(14)	0.13(1)	0.10(1)	0.05(1)	-0.02(1)	0.01(1)	-0.07(1)
C(15)	0.11(1)	0.08(1)	0.07(1)	-0.022(8)	-0.03(1)	-0.04(1)
C(16)	0.10(1)	0.09(1)	0.06(1)	-0.035(8)	0.005(8)	-0.05(1)
O(17)	0.15(1)	0.092(8)	0.095(8)	-0.033(6)	0.008(7)	-0.057(8)
C(18)	0.10(1)	0.13(1)	0.08(1)	-0.06(1)	-0.005(9)	-0.02(1)
C(19)	0.10(1)	0.11(1)	0.12(1)	-0.03(1)	0.00(1)	-0.05(1)
C(20)	0.10(1)	0.09(1)	0.13(1)	-0.05(1)	-0.01(1)	-0.03(1)
C(21)	0.10(1)	0.13(1)	0.14(2)	-0.04(1)	-0.02(1)	-0.05(1)
C(22)	0.12(2)	0.12(1)	0.23(2)	-0.06(1)	-0.01(1)	-0.10(1)
C(23)	0.34(3)	0.15(2)	0.11(2)	-0.04(1)	-0.05(2)	-0.09(2)
C(24)	0.16(2)	0.19(2)	0.16(2)	0.00(2)	-0.03(2)	-0.11(2)
C(25)	0.10(1)	0.025(7)	0.07(1)	-0.014(7)	-0.019(8)	-0.029(8)
C(26)	0.10(1)	0.09(1)	0.041(9)	-0.016(8)	-0.027(9)	-0.009(9)
C(27)	0.10(1)	0.08(1)	0.040(8)	-0.014(8)	-0.018(8)	-0.04(1)
C(28)	0.08(1)	0.12(1)	0.13(2)	-0.08(1)	-0.02(1)	-0.03(1)
C(29)	0.11(1)	0.10(1)	0.041(9)	-0.011(8)	0.036(9)	-0.06(1)
C(30)	0.10(1)	0.08(1)	0.048(8)	-0.040(8)	-0.020(8)	-0.004(9)
O(31)	0.109(9)	0.108(8)	0.109(8)	-0.050(7)	0.009(6)	-0.068(7)
C(32)	0.10(1)	0.11(1)	0.08(1)	-0.04(1)	0.00(1)	-0.01(1)
C(33)	0.09(1)	0.12(1)	0.11(1)	-0.07(1)	0.02(1)	-0.03(1)
C(34)	0.09(1)	0.13(1)	0.11(1)	-0.08(1)	-0.01(1)	-0.02(1)
C(35)	0.12(2)	0.17(2)	0.13(2)	-0.09(1)	-0.02(1)	-0.03(1)
C(36)	0.13(2)	0.19(2)	0.18(2)	-0.13(2)	-0.05(2)	-0.01(2)
C(37)	0.14(2)	0.30(3)	0.23(3)	-0.15(3)	0.03(2)	-0.12(2)
C(38)	0.15(2)	0.25(3)	0.20(2)	-0.15(2)	0.01(2)	-0.07(2)

...Contd.

Table 3.9 continued...

Atom	U_{11}	U_{22}	U_{33}	U_{23}	U_{13}	U_{12}
C(39)	0.09(1)	0.06(1)	0.07(1)	-0.009(9)	-0.02(1)	-0.031(9)
C(40)	0.14(2)	0.10(1)	0.08(1)	-0.01(1)	-0.02(1)	-0.08(1)
C(41)	0.12(2)	0.11(1)	0.07(1)	-0.04(1)	0.03(1)	-0.04(1)
C(42)	0.09(1)	0.12(1)	0.07(1)	-0.05(1)	0.02(1)	-0.02(1)
C(43)	0.10(1)	0.14(1)	0.12(1)	-0.10(1)	0.00(1)	-0.05(1)
C(44)	0.11(2)	0.11(1)	0.11(1)	-0.06(1)	0.03(1)	-0.04(1)
C(45)	0.11(1)	0.09(1)	0.12(1)	-0.04(1)	0.03(1)	-0.06(1)
C(46)	0.12(1)	0.10(1)	0.12(1)	-0.05(1)	-0.01(1)	-0.04(1)
C(47)	0.10(1)	0.08(1)	0.16(2)	-0.03(1)	0.01(1)	-0.04(1)
C(48)	0.13(1)	0.07(1)	0.11(1)	-0.031(9)	0.00(1)	-0.03(1)
C(49)	0.07(1)	0.07(1)	0.15(2)	0.02(1)	0.00(1)	-0.02(1)
C(50)	0.14(2)	0.11(2)	0.12(1)	-0.04(1)	-0.02(1)	-0.03(1)
C(51)	0.13(2)	0.08(1)	0.24(2)	0.00(1)	-0.01(1)	-0.06(1)
C(52)	0.06(1)	0.08(1)	0.08(1)	-0.014(9)	0.000(8)	-0.043(9)
C(53)	0.12(1)	0.11(1)	0.08(1)	-0.01(1)	0.00(1)	-0.06(1)
C(54)	0.19(2)	0.13(1)	0.09(1)	-0.05(1)	-0.01(1)	-0.10(1)
C(55)	0.13(1)	0.13(2)	0.04(1)	-0.01(1)	-0.01(1)	-0.04(1)
C(56)	0.14(2)	0.06(1)	0.09(1)	0.003(9)	0.00(1)	-0.05(1)
C(57)	0.10(1)	0.11(1)	0.11(2)	-0.04(1)	0.00(1)	-0.05(1)
C(58)	0.20(2)	0.19(2)	0.034(9)	-0.03(1)	-0.01(1)	-0.12(2)
C(59)	0.12(2)	0.15(2)	0.12(1)	-0.08(1)	0.00(1)	-0.04(1)
C(60)	0.14(2)	0.20(2)	0.10(1)	-0.08(1)	-0.02(1)	-0.04(2)
C(61)	0.10(1)	0.14(2)	0.14(2)	-0.04(1)	-0.01(1)	-0.04(1)
C(62)	0.17(2)	0.20(2)	0.16(2)	-0.14(2)	-0.06(2)	0.03(2)
C(63)	0.24(3)	0.27(3)	0.24(3)	-0.16(2)	-0.04(2)	-0.13(2)
C(64)	0.22(3)	0.28(3)	0.20(2)	-0.15(2)	-0.07(2)	0.01(2)

Table 3.10: Fractional coordinates and U_{iso}($\AA^2$) values of hydrogen atoms

Atom	x	y	z	U_{iso}	Atom	x	y	z	U_{iso}
H(6)	0.4411	0.2644	0.6484	0.08	H(362)	0.0482	0.7023	0.8127	0.14
H(9)	0.7677	0.4954	0.1436	0.08	H(371)	0.0481	0.6652	0.9543	0.20
H(16)	0.7889	0.5605	0.3590	0.07	H(372)	0.8815	0.7384	0.9551	0.20
H(15)	0.9348	0.6696	0.3318	0.09	H(451)	0.0776	-0.0257	0.6577	0.11
H(13)	0.0214	0.6952	0.0799	0.10	H(452)	0.2339	-0.1058	0.6861	0.11
H(12)	0.8784	0.5848	0.1103	0.08	H(461)	0.2917	-0.1030	0.5487	0.10
H(26)	0.4846	0.2911	0.7288	0.09	H(462)	0.1361	-0.0163	0.5162	0.10
H(27)	0.5339	0.3457	0.8195	0.07	H(471)	-0.0027	-0.1255	0.6186	0.12
H(29)	0.7482	0.5354	0.6192	0.07	H(472)	0.1525	-0.2118	0.6509	0.12
H(30)	0.6887	0.4796	0.5298	0.07	H(481)	0.2096	-0.2087	0.5130	0.10
H(40)	0.3313	0.1701	0.6776	0.10	H(482)	0.0575	-0.1227	0.4805	0.10
H(41)	0.1992	0.0548	0.7180	0.10	H(491)	-0.0852	-0.2342	0.5825	0.11
H(43)	0.3084	0.0403	0.4845	0.10	H(492)	0.0661	-0.3196	0.6136	0.11
H(44)	0.4335	0.1560	0.4436	0.10	H(501)	0.1223	-0.3116	0.4731	0.14
H(53)	0.5757	0.2447	0.2585	0.10	H(502)	-0.0268	-0.2297	0.4439	0.14
H(54)	0.5294	0.1914	0.1600	0.11	H(581)	0.6566	0.2441	-0.0256	0.13
H(56)	0.6357	0.4254	-0.0373	0.09	H(582)	0.5255	0.3403	-0.0583	0.13
H(57)	0.6818	0.4826	0.0601	0.09	H(591)	0.3642	0.2568	0.0413	0.12
H(181)	0.1429	0.7216	0.2921	0.11	H(592)	0.4987	0.1586	0.0718	0.12
H(182)	0.9856	0.8102	0.2705	0.11	H(601)	0.5408	0.1712	-0.0739	0.14
H(191)	0.1107	0.9158	0.1559	0.13	H(602)	0.3991	0.2621	-0.0985	0.14
H(192)	0.2705	0.8260	0.1801	0.13	H(611)	0.2489	0.1576	0.0038	0.12
H(201)	0.2350	0.8210	0.3209	0.10	H(612)	0.3854	0.0695	0.0301	0.12
H(202)	0.0839	0.9153	0.2922	0.10	H(621)	0.4221	0.0688	-0.1081	0.15
H(211)	0.2335	0.0095	0.1802	0.12	H(622)	0.2802	0.1628	-0.1370	0.15
H(212)	0.3818	0.9171	0.2203	0.12	H(631)	0.1271	0.0668	-0.0269	0.20
H(221)	0.1730	0.0154	0.3169	0.12	H(632)	0.2642	-0.0241	0.0044	0.20
H(222)	0.3795	0.9931	0.3001	0.12	H(241)	0.4791	0.0836	0.3305	0.16
H(231)	0.4040	0.0604	0.1965	0.15	H(242)	0.3519	0.1446	0.2605	0.16
H(232)	0.3483	0.0064	0.3181	0.15	H(243)	0.3037	0.0977	0.3658	0.16
H(321)	0.6823	0.6080	0.7154	0.10	H(381)	0.0601	0.8146	0.9455	0.16
H(322)	0.8432	0.5233	0.7246	0.10	H(382)	0.1356	0.7977	0.8561	0.16
H(331)	0.8353	0.4916	0.8710	0.10	H(383)	0.9701	0.8704	0.8569	0.16
H(332)	0.6701	0.5724	0.8646	0.10	H(511)	-0.0584	-0.3846	0.4697	0.15
H(341)	0.7705	0.6977	0.7678	0.11	H(512)	-0.0139	-0.4285	0.5705	0.15
H(342)	0.9348	0.6183	0.7654	0.11	H(513)	-0.1678	-0.3440	0.5405	0.15
H(351)	0.9457	0.5741	0.9129	0.11	H(641)	0.1316	-0.0453	-0.0763	0.21
H(352)	0.7815	0.6544	0.9150	0.11	H(642)	0.1541	0.0577	-0.1583	0.21
H(361)	0.8832	0.7835	0.8093	0.14	H(643)	0.2965	-0.0366	-0.1258	0.21

thermal vibrations than the core. Such a difference between the two sets of phenyl rings could be attributed to the substitution of the heptyloxy chains to the phenyl rings A and B and the substitution of the less heavy heptyl chains at the phenyl rings C and D *i.e.*, less heavy the substitution, higher is the thermal parameter of the phenyl ring. The average U_{eq} values of the chains A, B, C and D *viz.*, 0.13(3), 0.13(4), 0.12(2) and 0.16(4)Å^2 are also significantly higher than that of the core. Table 3.8 also shows that as could be anticipated, the thermal parameters of atoms close to the termini of chains are the highest. This feature is shown in the ORTEP diagram (Figure 3.2) where the thermal ellipsoids for the nonhydrogen atoms are plotted with 50% probability.

3.4.1 Molecular conformation

Figure 3.2 shows the atomic numbering scheme. From simple geometric considerations of molecular stability, it would appear that the chemically identical chains assume a *trans* arrangement with respect to the core. Interestingly, in the crystal structure, they are found to be *cis* (Figure 3.3). This result, though unexpected is *conclusive*. In the crystal structure of bis[1-thia-4-7-diaza cyclononane]cobalt(III) [Hambley *et* al, 1989], which is not mesogenic, molecular mechanics calculations have shown that the *cis* isomer is more stable than the corresponding *trans* isomer. Therefore, it appears that the occurrence of a stable *cis* form in crystals is not an uncommon feature. It must also be mentioned that in the case of a palladium β-diketone complex with dissimilar substitutions, two crystalline modifications corresponding to both *cis* and *trans* arrangements are reported [Okeya *et al*, 1981]. It is therefore not unlikely that in the case of Cu-

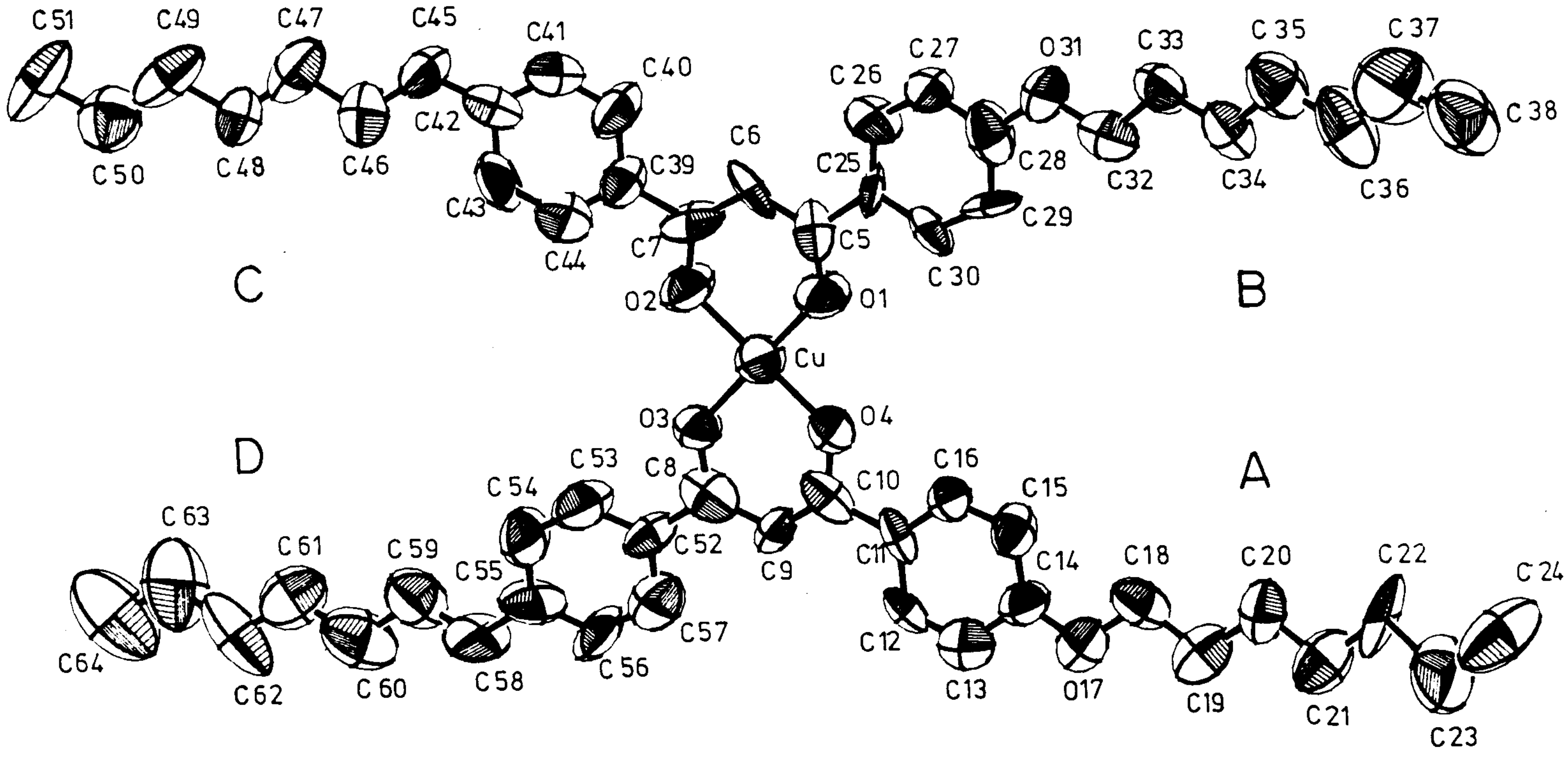

Figure 3.2: ORTEP diagram of the thermal ellipsoids drawn with 50% probability.

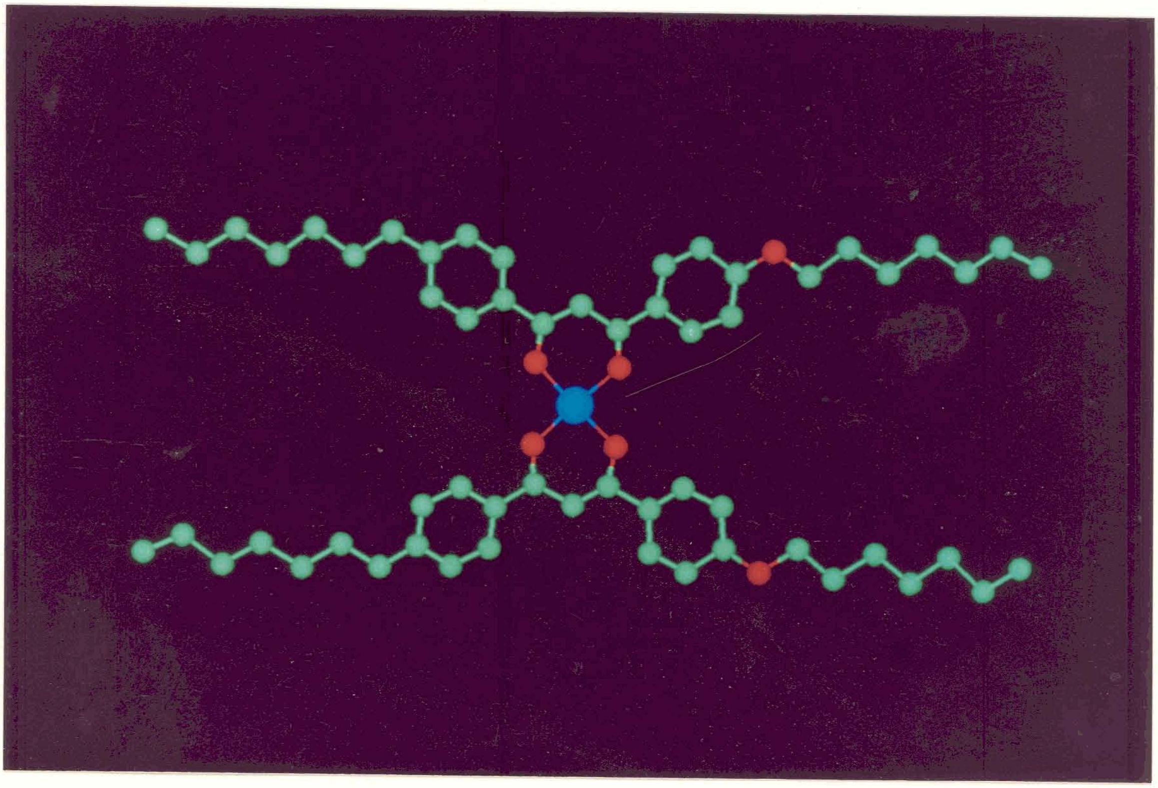

Figure 3.3: Conformation of the molecule.

OC_7H_{15}-C_7H_{15} also, a second crystalline modification with trans isomer exists. Examination of the crystallization dish has shown that there are in fact crystals with three different morphologies. Figure 3.4 includes the photographs of the three morphologically distinct forms, *viz.*, prismatic, needle-like and platy type of crystals. Of these, the prismatic and the platy crystals are more abundant than the needle-like crystals. The crystal structure described in this chapter is for the prismatic form. It is proposed to examine the other two forms of crystals also, to find out if either of them corresponds to the *trans* conformation.

It must also be mentioned that in the crystal structures of bis [1-phenyl-1,3-butanedionato] copper [Hon el al, 1966], copper(II) ethyl acetoacetate [Barclay and Cooper, 1965], bis {1-[4-trans-(4-propylcyclohexyl) phenyl]-octylpropane-1,3-dionato} copper(II) and bis{1-[4-*trans*-(4-propylcyclohexyl) phenyl]-methyl propane-1,3-dionato} copper(II) [Mühlburger and Haase, 1989], with dissimilar substitutions, only a *trans* arrangement has been reported. Our observations suggest that for these crystals also, the formation of a second crystalline modification corresponding to the cis form cannot be ruled out.

3.4.2 Molecular geometry

Tables 3.11(a) and (11) list the bond lengths and valence angles respectively. Average values of the bond lengths and bond angles in the core, phenyl rings and chains are presented in Table 3.11(c). Comparison with the values quoted by Allen et *al*, [1987], has also been included in Table 3.11(c).

Figure 3.5 represents the stereo view of the molecules in the unit cell. It is

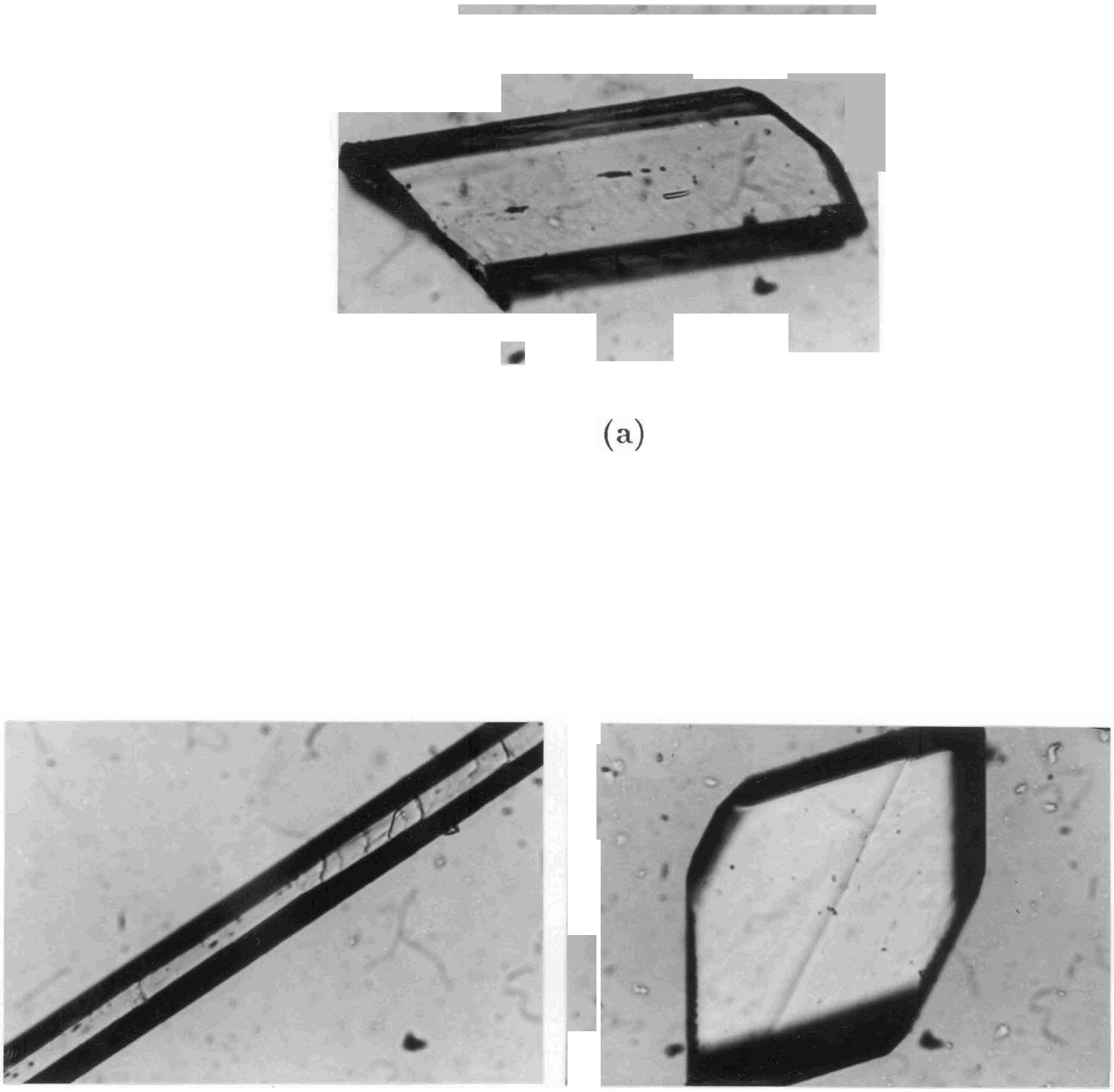

(a)

(b)

(c)

Figure 3.4: Three morphologically distinct forms. (a) prismatic (b) needle-like (c) platy.

Table 3.11(a): Bond lengths(Å).

Cu-O(1)	1.87(1)	C(28)-O(31)	1.40(3)
Cu-O(3)	1.89(1)	C(29)-C(30)	1.37(3)
Cu-O(4)	1.90(1)	O(31)-C(32)	1.44(2)
Cu-O(2)	1.93(1)	C(32)-C(33)	1.55(3)
O(1)-C(5)	1.23(2)	C(33)-C(34)	1.54(2)
O(2)-C(7)	1.27(2)	C(34)-C(35)	1.52(3)
O(3)-C(8)	1.30(2)	C(35)-C(36)	1.55(3)
O(4)-C(10)	1.30(2)	C(36)-C(37)	1.40(4)
C(5)-C(6)	1.45(2)	C(37)-C(38)	1.46(4)
C(5)-C(25)	1.47(3)	C(39)-C(40)	1.35(2)
C(6)-C(7)	1.38(3)	C(39)-C(44)	1.38(3)
C(7)-C(39)	1.53(2)	C(40)-C(41)	1.38(3)
C(8)-C(9)	1.45(2)	C(41)-C(42)	1.36(3)
C(8)-C(52)	1.49(3)	C(42)-C(43)	1.41(2)
C(9)-C(10)	1.30(3)	C(42)-C(45)	1.44(3)
C(10)-C(11)	1.56(2)	C(43)-C(44)	1.40(3)
C(11)-C(16)	1.29(3)	C(45)-C(46)	1.47(3)
C(11)-C(12)	1.42(2)	C(46)-C(47)	1.54(3)
C(12)-C(13)	1.36(3)	C(47)-C(48)	1.49(3)
C(13)-C(14)	1.45(3)	C(48)-C(49)	1.56(3)
C(14)-C(15)	1.37(2)	C(49)-C(50)	1.48(3)
C(14)-O(17)	1.37(2)	C(50)-C(51)	1.53(3)
C(15)-C(16)	1.40(3)	C(52)-C(53)	1.39(3)
O(17)-C(18)	1.48(2)	C(52)-C(57)	1.39(2)
C(18)-C(19)	1.53(3)	C(53)-C(54)	1.38(3)
C(19)-C(20)	1.56(3)	C(54)-C(55)	1.36(2)
C(20)-C(21)	1.51(3)	C(55)-C(56)	1.37(3)
C(21)-C(22)	1.50(3)	C(55)-C(58)	1.40(3)
C(22)-C(23)	1.59(3)	C(56)-C(57)	1.38(3)
C(23)-C(24)	1.40(4)	C(58)-C(59)	1.45(3)
C(25)-C(26)	1.37(2)	C(59)-C(60)	1.47(3)
C(25)-C(30)	1.37(2)	C(60)-C(61)	1.54(3)
C(26)-C(27)	1.32(3)	C(61)-C(62)	1.42(4)
C(27)-C(28)	1.42(2)	C(62)-C(63)	1.57(4)
C(28)-C(29)	1.39(2)	C(63)-C(64)	1.37(5)

Table 3.11(b): Bond angles(°).

O(1)-Cu-O(3)	177.6(4)
O(1)-Cu-O(4)	86.2(4)
O(1)-Cu-O(2)	92.8(4)
O(3)-Cu-O(4)	92.3(4)
O(3)-Cu-O(2)	88.7(4)
O(4)-Cu-O(2)	178.3(4)
C(5)-O(1)-Cu	129(1)
C(7)-O(2)-Cu	125.4(9)
C(8)-O(3)-Cu	128(1)
C(10)-O(4)-Cu	126(1)
O(1)-C(5)-C(6)	125(2)
O(1)-C(5)-C(25)	119(1)
C(6)-C(5)-C(25)	116(1)
C(7)-C(6)-C(5)	121(1)
O(2)-C(7)-C(6)	126(1)
O(2)-C(7)-C(39)	111(1)
C(6)-C(7)-C(39)	123(1)
O(3)-C(8)-C(9)	122(1)
O(3)-C(8)-C(52)	116(1)
C(9)-C(8)-C(52)	122(1)
C(10)-C(9)-C(8)	123(1)
C(9)-C(10-O(4)	128(2)
C(9)-C(10)-C(11)	122(1)
O(4)-C(10)-C(11)	110(1)
C(16)-C(11)-C(12)	121(1)
C(16)-C(11)-C(10)	119(1)
C(12)-C(11)-C(10)	120(1)
C(13)-C(12)-C(11)	119(1)
C(12)-C(13)-C(14)	120(2)
C(15)-C(14)-O(17)	129(1)
C(15)-C(14)-C(13)	118(2)
O(17)-C(14)-C(13)	113(1)
C(14)-C(15)-C(16)	119(1)
C(11)-C(16)-C(15)	123(1)
C(14)-O(17)-C(18)	114(1)
O(17)-C(18)-C(19)	109(1)
C(18)-C(19)-C(20)	110(1)
C(21)-C(20)-C(19)	110(1)
C(22)-C(21)-C(20)	107(1)
C(21)-C(22)-C(23)	102(2)
C(24)-C(23)-C(22)	105(2)
C(26)-C(25)-C(30)	117(1)
C(26)-C(25)-C(5)	129(1)
C(30)-C(25)-C(5)	114(1)
C(27)-C(26)-C(25)	124(1)
C(26)-C(27)-C(28)	119(1)
C(29)-C(28)-O(31)	128(1)
C(29)-C(28)-C(27)	120(1)
O(31)-C(28)-C(27)	112(1)
C(30)-C(29)-C(28)	117(1)
C(29)-C(30)-C(25)	124(1)
C(28)-O(31)-C(32)	114(1)
O(31)-C(32)-C(33)	108(1)
C(34)-C(33)-C(32)	111(1)
C(35)-C(34)-C(33)	110(1)
C(34)-C(35)-C(36)	109(2)
C(37)-C(36)-C(35)	110(2)
C(36)-C(37)-C(38)	116(2)
C(40)-C(39)-C(44)	116(2)
C(40)-C(39)-C(7)	123(1)
C(44)-C(39)-C(7)	121(1)
C(39)-C(40)-C(41)	122(2)
C(42)-C(41)-C(40)	125(2)
C(41)-C(42)-C(43)	113(2)
C(41)-C(42)-C(45)	127(2)
C(43)-C(42)-C(45)	119(2)
C(44)-C(43)-C(42)	122(2)
C(39)-C(44)-C(43)	122(2)
C(42)-C(45)-C(46)	120(2)
C(45)-C(46)-C(47)	114(1)
C(48)-C(47)-C(46)	111(1)
C(47)-C(48)-C(49)	114(1)
C(50)-C(49)-C(48)	117(2)
C(49)-C(50)-C(51)	118(2)
C(53)-C(52)-C(57)	116(2)
C(53)-C(52)-C(8)	119(1)
C(57)-C(52)-C(8)	125(1)
C(54)-C(53)-C(52)	123(2)
C(55)-C(54)-C(53)	120(2)
C(54)-C(55)-C(56)	117(2)
C(54)-C(55)-C(58)	124(2)
C(56)-C(55)-C(58)	119(2)
C(55)-C(56)-C(57)	123(2)
C(56)-C(57)-C(52)	120(2)
C(55)-C(58)-C(59)	121(2)
C(58)-C(59)-C(60)	119(2)
C(59)-C(60)-C(61)	119(2)
C(62)-C(61)-C(60)	121(2)
C(61)-C(62)-C(63)	115(2)
C(64)-C(63)-C(62)	120(2)

Table 3.11) Average values of bond lengths(Å) and valence angles(°) along with the values given by Allen *et al*, [1987].

	average bond lengths	values of Allen *et al*		average bond angles
Core:				
Cu-O	1.90(2)		O-Cu-O	92.6(3)
O-C_{ar}(core)	1.28(3)		**Cu-O-C_{ar}**	127(2)
C_{ar}-C_{ar} (core)	1.40(6)		O-C_{ar}-C_{ar}	126(2).
			C_{ar}-C_{ar}-C_{ar}	122(1)
Phenyl ring:				
A	1.38(5)	1.380(13)		120(2)
B	1.37(3)			120(3)
C	1.38(2)			120(4)
D	1.38(1)			120(3)
Chain:				
A	1.54(3)	1.530(15)		107(3)
B	1.51(6)			111(2)
C	1.51(4)			115(2)
D	1.49(6)			119(2)
O-C_{sp^3}	1.46(2)	1.450(14)	C_{phenyl}-O-C_{sp^3}	114(1)
O-C_{phenyl}	1.39(2)	1.370(11)	C_{phenyl}-C_{sp^3}-C_{sp^3}	120.5(5)
C_{sp^3}-C_{phenyl}	1.42(2)	1.513(14)		
C_{core}-C_{phenyl}	1.51(3)			

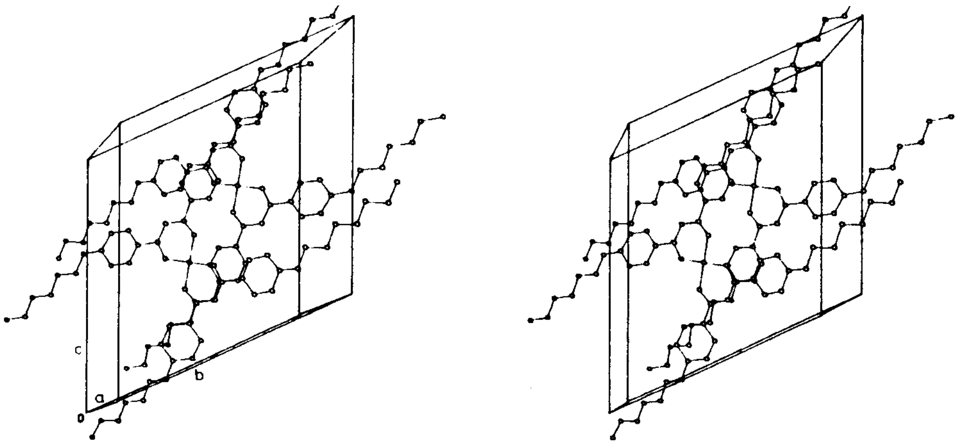

Figure 3.5: Stereo view of the molecules viewed down the a-axis.

found that all the four chains are fully extended in an all-trans conformation. The torsional angles indicating the trans conformation are listed in Table 3.12. Figure 3.6 shows the arrangement of oxygen atoms around the copper atom. The coordination is nearly square planar. As mentioned in the case of Cu-OC$_8$H$_{17}$, the distances O(1)...O(2), O(3)...O(4) are larger than the distances O(1)...O(4), O(2)...O(3). This feature confers a rectangular character to the coordination polyhedron formed by the oxygen atoms. It is also observed that the rectangle itself is quite distorted, *i.*e., the O(1)...O(4) distance is significantly shorter than the distance O(2)...O(3) (Figure 3.6). Conspicuously, the former, shorter distance falls on the side of the core where the oxyheptyl chains are present. This feature suggests that the shortening of the distance O(1)...O(4) could be due to the cis arrangement of the heptyloxy chains and possible interactions between the oxygen atoms in these chains.

The copper atom is significantly shifted displaced from the plane of the coordinating oxygen atoms, the displacement being 0.027(2)Å . Similar displacement of the metal atom from the plane of the coordinating oxygen atoms has been found in the crystal structures of bis [N-*p*-(*n*-hexyloxy)phenyl, **p**-(n-heptyloxy) salicylaldiminato] copper(II) [Roviello et *al*, 1988], bis [4-((4-butoxybenzoyl)-oxy)-*N*-(4- *n*-hexylphenyl) salicylaldiminato] copper(II) [Hoshino *et al*, 1990] and bis {1-[4-*trans*-(4-propylcyclohexyl) phenyl]-octylpropane-1,3-dionato} copper(II) [Mühlburger and Haase, 1989], which are also dissimilarly substituted.

As in the case of Cu-OC$_8$H$_{17}$, the 11-atom core of Cu-OC$_7$H$_{15}$-C$_7$H$_{15}$ is not strictly planar. The two halves of the core *viz.*, Cu, O(1), O(2), C(5) to C(7)

Table 3.12: Observed torsional angles(°) in the chains.

C(14)-O(17)-C(18)-C(19)	-175(1)
O(17)-C(18)-C(19)-C(20)	180(1)
C(18)-C(19)-C(20)-C(21)	177(1)
C(19)-C(20)-C(21)-C(22)	174(1)
C(28)-O(31)-C(32)-C(33)	-176(1)
O(31)-C(32)-C(33)-C(34)	-179(1)
C(32)-C(33)-C(34)-C(35)	-175(1)
C(33)-C(34)-C(35)-C(36)	-177(1)
C(34)-C(35)-C(36)-C(37)	179(2)
C(35)-C(36)-C(37)-C(38)	-176(2)
C(42)-C(45)-C(46)-C(47)	-176(2)
C(45)-C(46)-C(47)-C(48)	178(1)
C(46)-C(47)-C(48)-C(49)	179(1)
C(47)-C(48)-C(49)-C(50)	179(2)
C(48)-C(49)-C(50)-C(51)	180(2)
C(55)-C(58)-C(59)-C(60)	179(2)
C(58)-C(59)-C(60)-C(61)	176(2)
C(59)-C(60)-C(61)-C(62)	-178(2)
C(60)-C(61)-C(62)-C(63)	-179(2)
C(61)-C(62)-C(63)-C(64)	-176(2)

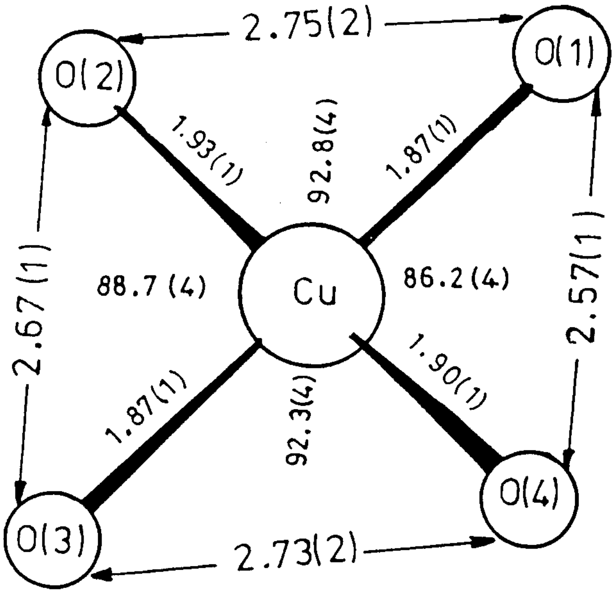

Figure 3.6: Coordination polyhedron around the copper atom.

and Cu, O(3), O(4), C(8) to C(10) are slightly tilted with respect to each other, the angle of tilt being 1.4". When the copper atom is not taken into consideration, the halves comprising of the atoms O(1), O(2), C(5), to C(7) and O(3), O(4), C(8) to C(10) are also only nearly planar, the angle between the normals to the above mentioned 5-atoms least squares planes being ~ 1°. Similar buckling has been observed in the crystal structures of bis{1-[4-*trans* -(4-propylcyclohexyl)phenyl]-octylpropane-1,3-dionato} copper(II) [Mühlburger and Haase, 1989], cis forms of bis [1-ethoxy-1,3-butanedionato] palladium(II) [Okeya *et al*, 1981] and bis[1-phenyl-1, 3-hexanedionato] palladium(II) [Fallon and Gatehouse, 1982] wherein the angle between the two halves of the core are ~ 3, 6 and 2° respectively.

In addition to the buckling between the two halves, each half of the core is itself found to be distorted. This distortion has been identified from the nonzero value of the angle between the least squares planes through the groups M-O-C-C in each half. The dihedral angle, η, between the least squares planes through the atoms Cu,O(1),C(5) and C(6) and Cu,O(2),C(7) and C(6) in one half of the core is 0.9°. The corresponding angle between the two planes fitted through the atoms Cu,O(3),C(8) and C(9) and Cu,O(4),C(10) and C(9) in the other half of the core is 2.5".

Figure 3.7 shows the displacements, δ's, of the atoms from the least squares plane through the 11-atom core. The planar phenyl rings A, B, C and D are tilted with respect to the core by 3, 2, 10 and 17° respectively. The tilts are controlled, primarily, by the steric interactions between the phenyl rings and

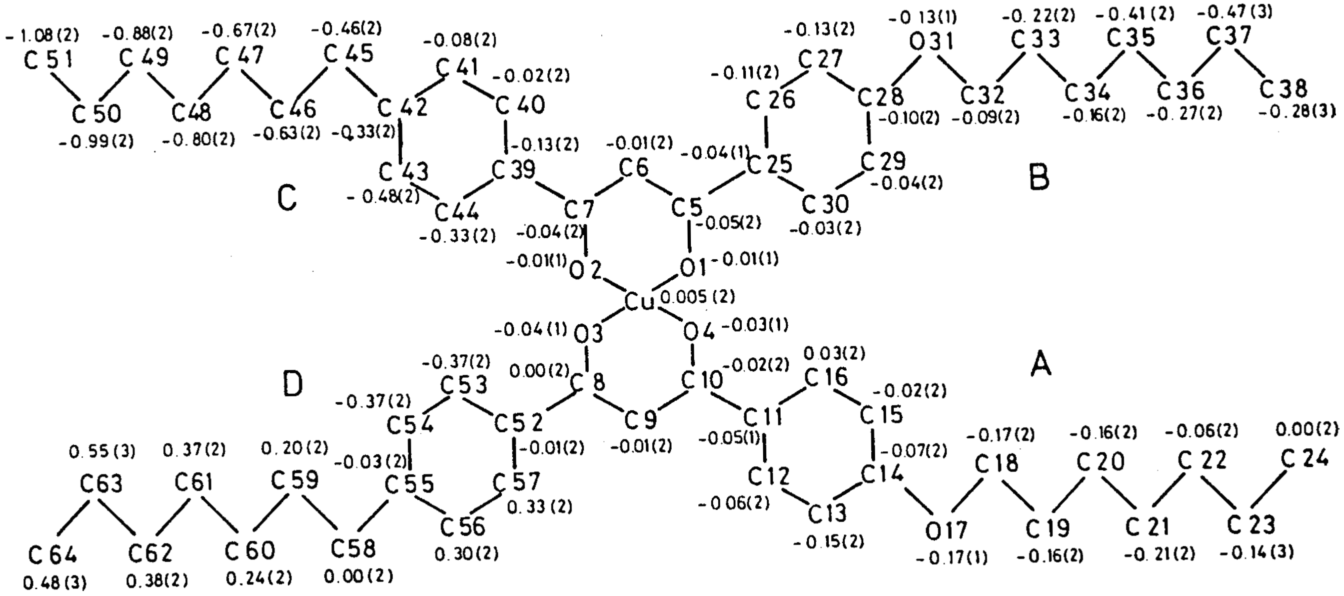

Figure 3.7': Displacements, δ's, of all the nonhydrogen atoms of the molecule from the plane through the 11-atom core.

the core atoms (Figure 3.8). Conspicuously, the tilts of the phenyl rings A and B substituted with heptyloxy chains are less than those of the rings C and D substituted with the less heavy heptyl chains. The chains A to D are inclined at 2, 9, 5 and 7° with respect to the core.

The end to end dimensions of the molecule calculated from the distances between the respective terminal atoms *viz.*, C(24)...C(64), C(38)...C(51), C(24)... C(38) and C(52)...C(64) are 28.5, 28.8, 9.94 and 10.62Å respectively. The slight asymmetry in the widths viz., 9.94 and 10.62Å respectively is a consequence of the difference in the lengths of the heptyl and the heptyloxy chains and their cis arrangement. The overall shape of the molecule, however, can be described as a slightly distorted rectangular disc with the length to width ratio of ~ 3, resembling the model B proposed by Ohta et *al* [1986] for $Cu\text{-}OC_8H_{17}$ in its mesophase.

Figure 3.9 shows the arrangement of the molecules in the plane perpendicular to the crystallographic a-axis. In the unit cell, although adjacent cores related by a centre of inversion, are well separated, the phenyl rings A and B of a molecule exhibit partial overlap over the phenyl rings of the centrosymmetrically related molecule. The overlapping phenyl rings are found to be those substituted with heptyloxy chains. The possible role of oxygen atoms in favouring the molecular overlap cannot therefore be ignored.

Examination of the intermolecular contact distances shows that the contact distances $\leq$ 4Å are conspicuously concentrated between the atoms of the centrosymmetrically related molecules in the unit cell (Table 3.13). These features

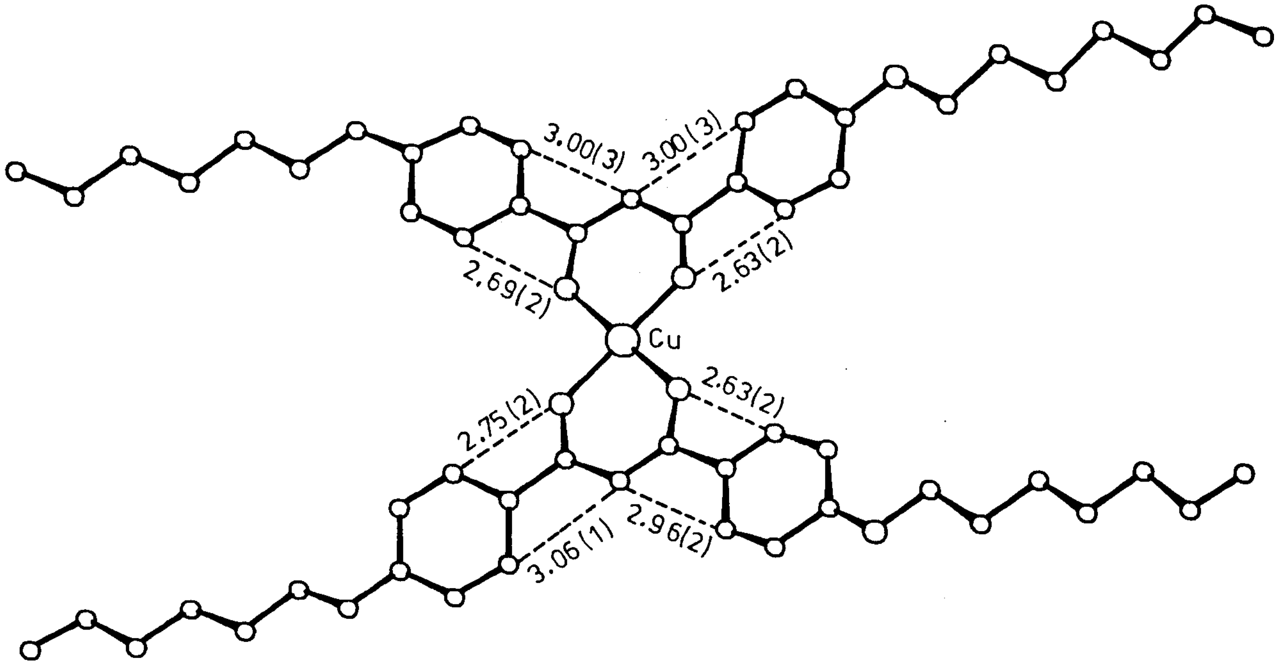

Figure **3.8:** Steric interactions controlling the tilts of the phenyl rings.

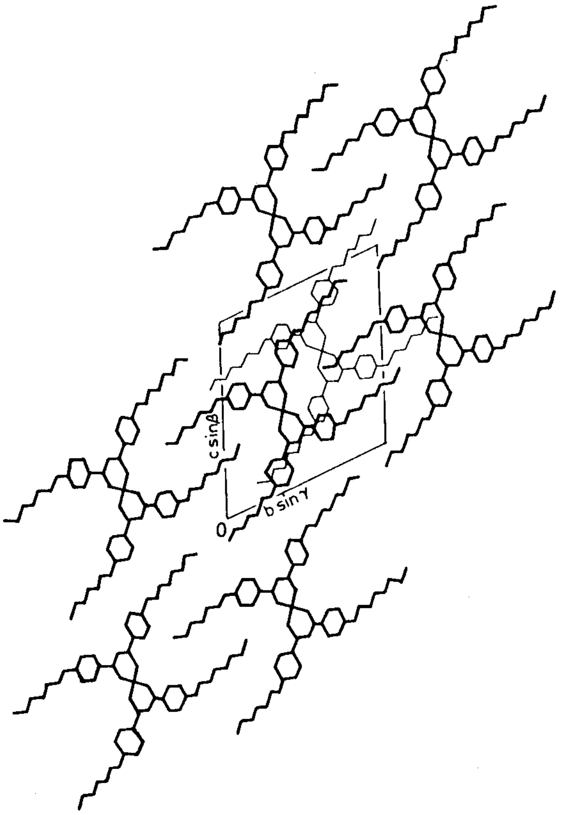

Figure **3.9:** Molecular arrangement perpendicular to the crystallographic a-axis.

Table 3.13: Nonbonded intermolecular contact distances between the centrosymmetrically related molecules in the unit cell. Distances less than the sum of the van der Waal's radii are marked with an asterisk.

Cu...C(29)	3.19(1)	O(4)...C(29)	3.87(2)
Cu...C(30)	3.38(1)	C(5)...C(30)	3.74(2)
Cu...C(28)	3.50(1)	C(8)...O(31)	3.34(2)
Cu...C(25)	3.83(1)	C(8)...C(28)	3.60(2)
Cu...C(27)	3.95(1)	C(8)...C(32)	3.81(2)
O(1)...C(30)	3.27(1)	C(8)...C(27)	3.88(2)
O(1)...C(25)	3.57(1)	C(9)...C(27)*	3.55(2)
O(1)...O(1)	3.76(1)	C(9)...C(28)	3.82(2)
O(1)...C(29)	3.78(2)	C(9)...O(31)	3.85(2)
O(1)...C(5)	3.83(2)	C(10)...C(27)*	3.35(2)
O(2)...C(29)	3.61(1)	C(10)...C(26)*	3.54(2)
O(3)...O(31)	3.40(1)	C(10)...C(28)	3.85(2)
O(3)...C(28)	3.42(2)	C(11)...C(26)	3.81(2)
O(3)...C(32)	3.55(2)	C(11)...C(27)	3.96(2)
O(3)...C(29)	3.68(2)	C(16)...C(26)	3.80(2)
O(4)...C(26)	3.34(1)	O(31)...C(52)	3.67(2)
O(4)...C(27)	3.43(1)	C(32)...C(52)	3.88(2)
O(4)...C(25)	3.50(2)	C(32)...C(53)	4.00(2)
O(4)...C(28)	3.71(2)	C(33)...C(53)	3.78(2)
O(4)...C(30)	3.76(2)	C(33)...C(52)	3.86(2)

suggest that the centrosymmetrically related molecules tend to pair, primarily, by van der Waal's interactions and perhaps to some extent by partial π-electron overlap. Each of the centrosymmetrically related pairs is surrounded by four others situated at $\pm b$ and $\pm$c respectively from the reference pair. A molecular coordination number of four is indeed not representative of a close packed arrangement [Gavezotti, 1989]. It may be mentioned that the pairing of the centrosymmetrically related molecules was earlier observed by us in the crystal structure of the discogen Cu-OC_8H_{17} where the cores of the pair exhibit substantial overlap. It must be pointed out that both the complexes which exhibit pairing within the unit cell are characterized by the presence of oxygen atoms around the core. Although any conclusion based on two observations is not reliable, it is perhaps not inappropriate to suggest that such pairing of molecules may be connected with the presence of oxygen atoms in the fringe. Figure 3.10 shows the layer-like arrangement of the molecules.

In the crystal structure, a striking concentration of aromatic groups occurs around the inversion centre at $\frac{1}{2}, \frac{1}{2}, \frac{1}{2}$. The pocket formed by the aromatic groups extends infinitely along the crystallographic a-direction and it includes the nonbonded interactions between the centrosymmetrically related molecules. A similar concentration of aliphatic chains is found around the inversion centre at 0,0,0 (Figure 3.5).

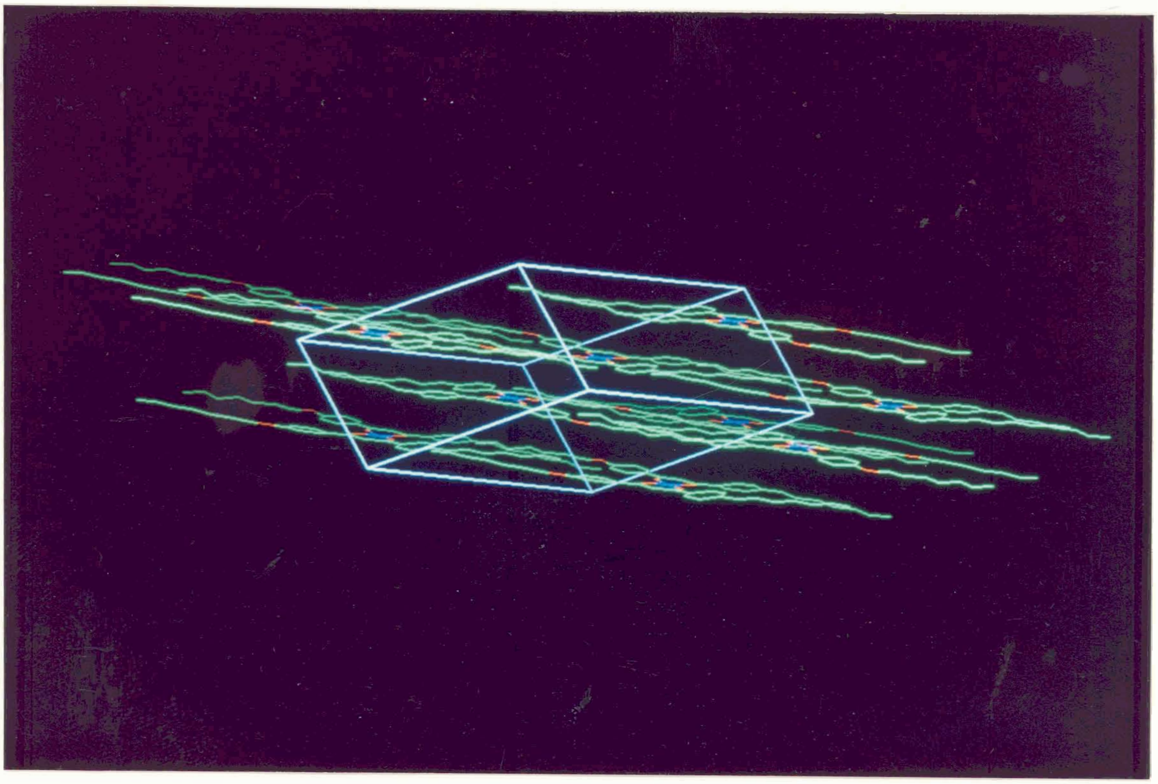

Figure 3.10: Layer-like arrangement of molecules.

3.5 Effect of molecular orientation on the most intense reflection $2\bar{2}0$

In the diffraction data from Cu-OC_7H_{15}-C_7H_{15}, the reflection $2\bar{2}0$ is most intense; the second most intense reflection being $\bar{1}03$ with $F_{\bar{1}03} = 0.43F_{2\bar{2}0}$. The high intensity of $2\bar{2}0$ is obviously an indication of the molecular orientation in the unit cell. As the crystal structure of Cu-OC_7H_{15}-C_7H_{15} was solved by direct methods, in a fairly straight forward manner, it was not necessary to adopt trial and error methods which often utilize information concerning the most intense reflections *etc.* However, after obtaining the structure solution, it was intersting to note that the intensity of $(2\bar{2}0)$ was controlled primarily by the fact that for most of the atoms, the value of (x-y) was $\sim$ 0.25. A brief summary of this observation is presented here.

In the space group $P\bar{1}$, the structure factor expression takes the form,

$$F_{hkl} = \sum_{j=1}^{N} f_j cos2\pi(hx_j + ky_j + lz_j) \qquad (3.1)$$

where f_j is the atomic scattering factor and x_j, y_j and z_j are the positional coordinates for.the j^{th} atom and N is the total number of atoms in the unit cell.

For $h\bar{h}0$ type of reflections, equation 3.1 takes the form,

$$F_{h\bar{h}0} = \sum_{j=1}^{N} f_j cos2\pi(hx_j + \bar{h}y_j) \qquad (3.2)$$

Then

$$F_{2\bar{2}0} = \sum_{j=1}^{N} f_j cos4\pi(x - y) \qquad (3.3)$$

which shows that when (x-y)=1/4, the structure factor gets the full contribution from all the atoms. (x-y)=1/2 also leads to full contribution of atoms to the structure factor, however, with opposite sign. Inspection of Table 3.8 shows that for most of the atoms, the value of (x-y) is close to 1/4, thereby leading to a high value of the structure factor of 220. The intensity of the higher order reflection $4\bar{4}0$, ($F_{4\bar{4}0}=0.23F_{2\bar{2}0}$) can also be explained in the same fashion. The comparatively low intensity of the reflection 660, $F_{6\bar{6}0}=0.03F_{2\bar{2}0}$ seems to be essentially due to the reduction in the scattering factor. It is found that $\frac{\sum f^2_{j_{6\bar{6}0}}}{\sum f^2_{j_{2\bar{2}0}}}$ is —0.27. After correcting for the thermal vibration, this ratio reduces further to ~0.1

In the case of $h\bar{h}0$ type of reflections with h odd, eg., $1\bar{1}0$, the structure factor expression becomes,

$$F_{1\bar{1}0} = \sum_{j=1}^{N} f_j cos 2\pi(x-y) \qquad (3.4)$$

with (x-y)~1/4, F tends to 0. The structure factors given in the Appendix do indeed show that the reflection $1\bar{1}0$ and its higher order reflections $3\bar{3}0$ and 550 are weak.